SHORT COMMUNICATION

WILEY

In vitro pharmacology of fentanyl analogs at the human mu opioid receptor and their spectroscopic analysis

Sherif H. Hassanien[1†] [ID] | Jonathon R. Bassman[1†] | Carmelita M. Perrien Naccarato[2] | Jack J. Twarozynski[2] | John R. Traynor[2,3] | Donna M. Iula[1] | Jessica P. Anand[2,3†] [ID]

[1]Cayman Chemical Co., Ann Arbor, Michigan

[2]Department of Pharmacology, University of Michigan, Ann Arbor, Michigan

[3]Edward F. Domino Research Center, University of Michigan, Ann Arbor, Michigan

Correspondence
Sherif H. Hassanien, Cayman Chemical Co., Ann Arbor, MI, 48108.
Email: sherifhh1191@live.com

Funding information
Cayman Chemical Company, Ann Arbor; Edward F. Domino Research Center, University of Michigan; National Institute on Drug Abuse, Grant/Award Numbers: DA039997, DA048129; Undergraduate Research Opportunity Program, University of Michigan

Abstract

Opioids are widely misused and account for almost half of overdose deaths in the United States. The cost in terms of lives, health care, and lost productivity is significant and has been declared a national crisis. Fentanyl is a highly potent mu opioid receptor (MOR) agonist and plays a significant role in the current opioid epidemic; fentanyl and its analogs (fentalogs) are increasingly becoming one of the biggest dangers in the opioid crisis. The availability of fentalogs in the illicit market is thought to play a significant role in the recent increase in opioid-related deaths. Although there is both rodent homolog *in vivo* and *in vitro* data for some fentalogs, prior to this publication very little was known about the pharmacology of many of these illicit compounds at the human MOR (hMOR). Using gas chromatography–mass spectrometry, nuclear magnetic resonance spectroscopy, and *in vitro* assays, this study describes the spectral and pharmacological properties of 34 fentalogs. The reported spectra and chemical data will allow for easy identification of novel fentalogs in unknown or mixed samples. Taken together these data are useful for law enforcement and clinical workers as they will aid in the identification of fentalogs in unknown samples and can potentially be used to predict physiological effects after exposure.

KEYWORDS

fentanyl, GC–MS, mu opioid receptor, opioid epidemic, pharmacology

1 | INTRODUCTION

Over the past decade, the medical, economic, and social cost of the opioid crisis has increased steadily in the United States (U.S.).[1–5] This increase is due, in part, to the increased number of opioid prescriptions written since the 1990s; one recent estimate states that almost 290 million opioid prescriptions are written in the U.S. annually.[6] In 2017, there were nearly 48,000 opioid related deaths in the U.S.,[7] which was more than the number of automobile accident fatalities.[8]

The opioid crisis was estimated to have cost the U.S. over $600 billion from 2015 to 2019.[9]

Initially, prescription opioid analgesics made up the majority of abused opioids, which was dubbed as the first wave of the opioid epidemic by the U.S. Centers for Disease Control and Prevention. However, after 2010, heroin became the largest contributor to opioid-related deaths, the second wave of the opioid epidemic, as opioid drug users transitioned away from prescription opioids as they became more difficult to acquire.[10] Recently, the third wave of the

opioid epidemic has emerged: synthetic opioids such as fentanyl have been found increasingly in the illicit drug supply, in heroin and false prescription opioid samples, and also in samples containing stimulants such as cocaine or amphetamine.[11] In addition to fentanyl, structurally related fentanyl analogs (fentalogs) have been used to adulterate illicit drug samples and, in some cases, have been administrated as the primary drug of use.[12–14] As a result, fentanyl is subject to core U.S. Drug Enforcement Administration scheduling, and all illicit fentanyl analogs are considered Schedule I compounds.

Clinically used opioid analgesics and illicit opioids all exert their physiological actions through the stimulation of the mu opioid receptor (MOR).[15–17] Agonist activity at MOR produces not only the clinically desirable analgesic properties of opioids, but also euphoria, a significant contributor to addiction, and respiratory depression, the presumed main cause of morbidity from opioid overdose.[18–20] Further, the elimination of MOR by knockout in rodents prevents morphine, a prototypical opioid agonist, from producing respiratory depression.[21] The kappa opioid receptor (KOR) and the delta opioid receptor (DOR) have not been shown to have significant influence on respiration.[21] It is noteworthy that fentanyl's ability to produce opioid-induced respiratory depression exceeds that of common painkillers such as morphine or other similar morphinan compounds.[22] Further, fentanyl is known to cause severe muscle rigidity, which likely exacerbates the acute toxicity of fentanyl and its analogs.[23] Although it is known that fentanyl is a potent agonist at rat, human, and marmoset MOR, most of the novel, illicit fentalogs in this investigation have no previously reported data at the human MOR (hMOR).

The clinical relevance of *in vitro* studies at the human opioid receptors cannot be overlooked. Over the past several decades, fentalogs have been pharmacologically characterized primarily in rodent models.[24–39] Much of the fentalog data collected in this area is represented by *in vivo* experiments in which pharmacokinetic parameters make comparative evaluation difficult. In these studies, the fentalogs displayed a wide range of ED_{50} values relative to fentanyl.[24] By comparison, *in vitro* data on fentalogs have been scarce, with few reports in recent decades.[31-41,] The use of brain homogenate and membrane preparations of rats have been classically the primary avenue for *in vitro* potency testing of fentalogs;[25,26,29,30] however, these studies often come with caveats, as these experiments do not examine direct effects at a single receptor, but are complicated by the presence of multiple receptors, metabolizing enzymes, and so on. By comparison, the use of cell lines overexpressing a single receptor, hMOR, for *in vitro* characterization of fentalogs has gone largely uninvestigated. Data at the human receptors (as opposed to those of rodent or other species) are valuable and have potential to more accurately reflect the effects of these compounds on human subjects.

In this report we characterize 34 fentalogs of interest (Figure 1; Table 1) for the forensic and law enforcement community using cell systems overexpressing hMOR and highlight their structure activity relationships (SAR). These samples were chosen to reflect compounds commonly requested by forensic laboratories as they likely represent those found in samples gathered in search and seizure by law enforcement. We report the affinities, agonist activity, and potencies of these
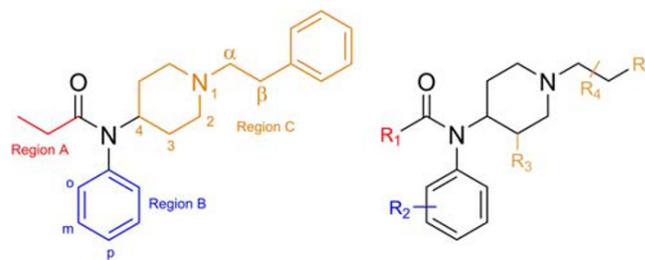

FIGURE 1 Structure of fentanyl (compound 1, left) with positional naming conventions and a generic fentanyl scaffold (right) displaying sites of modification (R1–R5)

fentanyl analogs at the hMOR, as well as their gas chromatography–mass spectrometry (GC–MS), nuclear magnetic resonance (NMR), and infrared (IR) spectral data. This novel data can be important to the law enforcement, emergency responder, and regulatory communities.

2 | MATERIALS AND METHODS

2.1 | Synthesis of fentalogs

2.1.1 | Materials

All solvents were purchased from Millipore Sigma (Burlington, MA, USA). Synthetic reagents were purchased from TCI America (Portland, OR, USA), Millipore Sigma , Asta-Tech Inc. (Bristol, PA, USA), Oakwood Chemicals (Estill, SC, USA), Alfa Aesar (Haverhill, MA, USA), and AK Scientific (Union City, CA, USA) and were used without further purification.

All compounds were synthesized using methods from previously reported synthetic work.[42,43] Chemical structures were determined using GC–MS, flow injection analysis mass spectrometry (FIA-MS), liquid chromatography–mass spectrometry (LC–MS), proton nuclear magnetic resonance spectroscopy (^{1}H-NMR), carbon nuclear magnetic resonance (^{13}C-NMR), infrared spectroscopy (FT-IR), and melting point. Purities were assessed using high-performance liquid chromatography (HPLC) and ^{1}H-NMR. All final compounds were purified to >98%, in accordance with industry standards. Synthesis methods and full characterization of compounds may be found in the supporting information section.

2.2 | Gas chromatography–mass spectrometry

2.2.1 | Sample preparation

Each compound was dissolved in HPLC-grade methanol (Sigma Aldrich, St. Louis, MO, USA) to produce a 1.0 mg/mL solution, of which 1.0 μL was used for sample injection.

2.2.2 | Instrumentation

All samples were characterized by GC–MS using an Agilent 6890 Gas chromatograph equipped with an Agilent 5973 Mass Selective

TABLE 1 Structural definition of compounds based on Figure 1

Name	Compound #	R1	R2	R3	R4	R5
Fentanyl	1	Ethyl	H	H	α-H, β-H	Phenyl
Cyclopropyl fentanyl	2	Cyclopropyl	H	H	α-H, β-H	Phenyl
p-Methyl cyclopropyl fentanyl	3	Cyclopropyl	p-Methyl	H	α-H, β-H	Phenyl
Cyclobutyl fentanyl	4	Cyclobutyl	H	H	α-H, β-H	Phenyl
Cyclopentyl fentanyl	5	Cyclopentyl	H	H	α-H, β-H	Phenyl
Furanyl fentanyl	6	2-Furanyl	H	H	α-H, β-H	Phenyl
Tetrahydrofuran fentanyl	7	2-Tetrahydrofuranyl	H	H	α-H, β-H	Phenyl
Acetyl fentanyl	8	Methyl	H	H	α-H, β-H	Phenyl
o-Methyl acetyl fentanyl	9	Methyl	o-Methyl	H	α-H, β-H	Phenyl
α-Methyl acetyl fentanyl	10	Methyl	H	H	α-Methyl, β-H	Phenyl
Acryl fentanyl	11	Ethylene	H	H	α-H, β-H	Phenyl
o-Fluoro acryl fentanyl	12	Ethylene	o-Fluoro	H	α-H, β-H	Phenyl
p-Fluoro acryl fentanyl	13	Ethylene	p-Fluoro	H	α-H, β-H	Phenyl
Isobutyryl fentanyl	14	Isopropyl	H	H	α-H, β-H	Phenyl
o-Fluoro isobutyryl fentanyl	15	Isopropyl	o-Fluoro	H	α-H, β-H	Phenyl
m-Fluoro isobutyryl fentanyl	16	Isopropyl	m-Fluoro	H	α-H, β-H	Phenyl
p-Fluoro isobutyryl fentanyl	17	Isopropyl	p-Fluoro	H	α-H, β-H	Phenyl
p-Chloro isobutyryl fentanyl	18	Isopropyl	p-Chloro	H	α-H, β-H	Phenyl
Pivaloyl fentanyl	19	Tert-butyl	H	H	α-H, β-H	Phenyl
Butyryl fentanyl	20	Propyl	H	H	α-H, β-H	Phenyl
o-Fluoro butyryl fentanyl	21	Propyl	o-Fluoro	H	α-H, β-H	Phenyl
Methoxyacetyl fentanyl	22	Methoxy methylene	H	H	α-H, β-H	Phenyl
o-Fluoro fentanyl	23	Ethyl	o-Fluoro	H	α-H, β-H	Phenyl
m-Fluoro fentanyl	24	Ethyl	m-Fluoro	H	α-H, β-H	Phenyl
p-Fluoro fentanyl	25	Ethyl	p-Fluoro	H	α-H, β-H	Phenyl
o-Methyl fentanyl	26	Ethyl	o-Methyl	H	α-H, β-H	Phenyl
m-Methyl fentanyl	27	Ethyl	m-Methyl	H	α-H, β-H	Phenyl
p-Methyl fentanyl	28	Ethyl	p-Methyl	H	α-H, β-H	Phenyl
p-Chloro fentanyl	29	Ethyl	p-Chloro	H	α-H, β-H	Phenyl
Cis-3-methyl fentanyl	30	Ethyl	H	Cis-methyl	α-H, β-H	Phenyl
Trans-3-methyl fentanyl	31	Ethyl	H	Trans-methyl	α-H, β-H	Phenyl
Furanylethyl fentanyl	32	Ethyl	H	H	α-H, β-H	2-Furan
β-Hydroxy thiofentanyl	33	Ethyl	H	H	α-H, β-OH	2-Thiophene
β-Methyl fentanyl	34	Ethyl	H	H	α-H, β-methyl	Phenyl

Detector (Santa Clara, CA, USA). The attached column was a Restek (Bellefonte, PA, USA), Rtx-5 MS, 30 m × 0.32 mm I.D., with 0.5 µm film thickness (phase composition: crossbond 5% diphenyl/95% dimethyl polysiloxane).

2.2.3 | Methods and parameters

The temperature of the injector was maintained at constant flow at 300°C. The oven temperature was started at 240°C for 1 min, then increased by 30°C/min to 300°C where holding time was 27 min (30 min total run time). Helium was used as the carrier gas at

2.0 mL/min (split ratio: 15:1). Mass spectrometer settings were as follows: transfer line, 300°C; MS source, 230°C; MS quad, 150°C; scan range, m/z 40–600; electron ionization, 70 eV. More details on the GC parameters can be found in the supporting information section.

2.3 | ^{1}H-NMR spectroscopy

2.3.1 | Sample preparation and instrumentation

Samples were prepared as ∼5 mg/mL solutions in deuterium-labeled chloroform (Acros Organics, Waltham, MA, USA), dimethylsulfoxide

(Cambridge Isotope Laboratories, Tewksbury, MA, USA), or methanol (CDN Isotopes, Pointe Claire, Canada). ^{1}H-NMR spectra were measured on a Varian Unity Inova 400 MHz spectrometer. Chemical shifts were reported in parts per million (ppm). Results can be found in the supporting information section.

2.4 | Melting point

2.4.1 | Sample preparation and instrumentation

Samples were prepared using neat solids and Kimble capillary tubes (1.5 × 90 mm). Melting point ranges were measured using an Electrothermal Digital Melting Point apparatus, using a 1°/min ramping method. Start temperature is the temperature at which the solid first begins to change from a dry solid; final temperature is the temperature at which the solid is completely melted to a homogeneous fluid. Results can be found in the supporting information section.

2.5 | Fourier-transform infrared spectroscopy

2.5.1 | Sample preparation and instrumentation

Samples were prepared as neat solids that were set directly on top of the detector. IR spectra were collected using a Perkin Elmer Spectrum 65 FT-IR spectrometer, and the data were reported in wavenumbers (cm^{-1}). Results can be found in the supporting information section.

2.6 | *In vitro* characterization of fentalogs

2.6.1 | Cell lines and membrane preparations

All tissue culture reagents were purchased from Gibco Life Sciences (Waltham, MA, USA), Fisher Scientific (Waltham, MA, USA), or Sigma-Aldrich unless otherwise noted. Radio-labeled ligands were purchased from Perkin Elmer (Waltham, MA, USA). Chinese hamster ovary (CHO) cells stably expressing a human μ (hMOR) in a pcDNA 3.1 vector using geneticin as the selection agent were used for all *in vitro* assays. These cells stably express hMOR at 4240 fmoles of receptor/mg of protein. This cell line was generously provided by Dr. Lawrence Toll.[44]

Cells were grown to confluence at 37°C in 5% CO$_2$ in Dulbecco's Modified Eagle's Medium: F12 Ham (1:1 mixture) containing 10% v/v fetal bovine serum and 5% v/v penicillin/streptomycin. Membranes were prepared by washing confluent cells thrice with ice-cold phosphate-buffered saline (0.9% NaCl, 0.61mM Na$_2$HPO$_4$, 0.38mM KH$_2$PO$_4$, pH 7.4). Cells were detached from the plates by incubation in warm harvesting buffer (20mM HEPES, 150mM NaCl, 0.68mM EDTA, pH 7.4) and pelleted by centrifugation at 200g for 3 min. The cell pellet was suspended in ice-cold 50mM Tris–HCl buffer (pH 7.4) and homogenized using a Tissue-Tearor (Biospec Products, Bartlesville, OK, USA) for 20 s at setting 4. The homogenate was centrifuged at 20,000g for 20 min at 4°C, and the pellet was rehomogenized in 50mM Tris–HCl (pH 7.4) using a Tissue-Tearor for 10 s at setting 2, followed by recentrifugation. The final pellet was resuspended in 50mM Tris–HCl (pH 7.4) and frozen in aliquots at −80°C. Protein concentration was determined via Pierce BCA protein assay kit using bovine serum albumin as the standard.

2.6.2 | Radioligand competition binding assays

Assays were performed using competitive displacement of 0.2nM [^{3}H]diprenorphine (250 μCi, 1.85TBq/mmol, K$_D$ at hMOR 0.38nM), a nonselective opioid ligand, by the test fentalog from membrane preparations stably expressing hMOR. The assay mixture, containing membranes (approximately 5 μg protein/tube) in 50mM Tris–HCl buffer (pH 7.4) [^{3}H]diprenorphine, and various concentrations of test fentalog, was incubated on a shaker at room temperature for 1 h to allow binding to reach equilibrium. The samples were filtered through Whatman GF/C filters and washed thrice with 50mM Tris–HCl buffer (pH 7.4). The radioactivity retained on dried filters was determined by liquid scintillation counting after saturation with EcoLume liquid scintillation cocktail in a 2450 MicroBeta2 (Perkin-Elmer). Nonspecific binding was determined using 10μM naloxone; total binding was determined using water. The results presented are the mean ± SEM from three individual assays performed on three different days. Each individual assay was performed in duplicate and then averaged. The data were fitted to a one-site, nonlinear regression curve (one-site competition binding curve) using GraphPad Prism v8.02; IC$_{50}$ values were converted to K$_i$ values using the Cheng-Prusoff equation.[45]

2.6.3 | Stimulation of GTPγ[^{35}S] binding

Agonist stimulation of [^{35}S]guanosine5'-O-[gamma-thio]triphosphate ([^{35}S]GTPγS, 1250 Ci, 46.2TBq/mmol) binding was measured. Membranes (10 μg of protein/tube) were incubated for 1 h at room temperature in GTPγS buffer (50mM Tris–HCl, 100mM NaCl, 10mM MgCl$_2$, 1mM EDTA, pH 7.4) containing 0.1nM [^{35}S]GTPγS, 30μM guanosine diphosphate (GDP), and varying concentrations of test fentalog. Test fentalog stimulation of [^{35}S]GTPγS was compared with 10μM standard MOR agonist [D-Ala^2, N-MePhe^4, Gly-ol]-enkephalin (DAMGO). The reaction was terminated by rapidly filtering through GF/C filters and washing five times with GTPγS buffer. Retained radioactivity was measured as described earlier. The results presented are the mean ± SEM from three individual assays performed on three different days. Each individual assay was performed in duplicate and then averaged. The data were fitted to a nonlinear regression curve (sigmoidal dose response curve for agonist stimulation) using GraphPad Prism v8.02.

2.6.4 | Data collection

All *in vitro* assays were run in duplicate in three or more individual assays. Data are presented as the mean ± SEM for all data points.

Data for all *in vitro* competition binding assays are normalized such that basal (in the presence of 10μM naloxone) and total binding (in the absence of any drug) is set to 0% and 100% binding, respectively. Data for all *in vitro* [^{35}S]GTPγS assays are normalized such that basal (in the absence of drug) and total binding (in the presence of 10μM standard agonist DAMGO) is set to 0% and 100% stimulation, respectively. This normalization is used to account for variations between membrane preparations or assays.

3 | RESULTS AND DISCUSSION

3.1 | *In vitro* pharmacological data: Agonist binding affinity and efficacy at hMOR

The binding affinity (K_i) and agonist efficacy (% stimulation and EC$_{50}$) of 34 fentalogs were determined at hMOR (Table 2). Competition binding assay using [^{3}H]diprenorphine and membranes stably over-expressing hMOR was used to determine binding affinity of fentalogs. The [^{35}S] GTPγS binding assay was used to determine efficacy data in terms of % max stimulation and potency (EC$_{50}$) relative to the standard agonist DAMGO. Using these data, the SAR of all 34 fentalogs was compared. As a point of comparison, morphine was also tested: K_i 4.2 ± 0.13nM, % stimulation 99 ± 4%, EC$_{50}$ 150 ± 50nM.

As expected, fentanyl (**1**) displayed tight binding (1.6 ± 0.4nM) and full agonist activity (89 ± 9% of DAMGO, a prototypical MOR agonist) at hMOR. This is consistent with previous studies of fentanyl at both the human and marmoset MOR.[46,47]

Modifications at Region A (**2–22**, Table 2) sampled both constrained (**2–7**) and flexible moieties (**8–22**). In general, the majority of these compounds displayed single-digit nanomolar affinity for hMOR, with a few notable exceptions. Acetyl fentanyl (**8**), which contains only a methyl group in Region A, has much lower affinity for the hMOR (64nM) as compared to fentanyl (**1**, 1.6nM). Similarly, analogs **9** and **10** (also a methyl in Region A) display weaker binding at hMOR (K_i: 43 and 19nM, respectively). This suggests that Region A has minimum bulk requirements to maintain optimal contact with the orthosteric binding site of hMOR. There is, however, some flexibility in terms of how large a group can be accommodated in Region A; the four-carbon *tert*-butyl group (**19**) and the five-carbon cyclopentyl group (**5**) both bind well to hMOR (4.5 and 6.6nM, respectively). Although increased bulk at R1 had little effect on binding affinity when increasing ring size (**2**, **4**, and **5**), a large difference in EC$_{50}$ potency was observed (55, 160, and 600 nM, respectively).

The presence of an oxygen atom in Region A seems to affect binding. One example is tetrahydrofuran fentanyl (**7**) that displays decreased binding affinity (31nM) at the hMOR relative to cyclopentyl fentanyl (**5**) (6.6nM). The EC$_{50}$ of **7** (390nM) was 12-fold less potent than fentanyl (**1**) (32nM), and the G protein simulation was decreased to 36%. Another direct comparison can be made between methoxyacetyl fentanyl (**22**) (17nM) and butyryl fentanyl (**20**) (3.5nM). Compound **22** with non-aromatized lone pairs of electrons displayed decreased binding at hMOR, which could suggest that hydrogen bond

TABLE 2 *In vitro* binding affinity and efficacy data at hMOR for fentalogs with modifications at Region A or Regions A and B (2-22), Region B (23-29), and Region C (30-34)

Compound #	Binding affinity K$_i$ nM (SEM)	Efficacy % stimulation (SEM)	EC50 nM (SEM)
Fentanyl (1)	1.6 (0.4)	89 (9)	32 (8)
2	2.4 (0.4)	75 (6)	55 (10)
3	7.2 (1.7)	61 (4)	>1000
4	5 (1)	41 (5)	160 (30)
5	6.6 (0.7)	56 (5)	600 (190)
6	1.3 (0.07)	20.4 (2.9)	9.3 (1.9)
7	31 (6)	36 (2)	390 (96)
8	64 (15)	49 (6)	>2000
9	43 (10)	43 (2)	>1000
10	19 (3)	53 (7)	>500
11	2.1 (0.04)	77.9 (1.4)	68 (16)
12	1.1 (0.5)	81 (6)	14 (1)
13	4.3 (0.9)	82 (12)	84 (11)
14	6.6 (1.3)	96 (11)	137 (13)
15	1.3 (0.02)	102 (7)	42 (13)
16	4.5 (0.4)	95 (12)	>500
17	24 (4)	82 (16)	>1000
18	82 (17)	>65	>2000
19	4.5 (0.7)	64 (8)	531 (136)
20	3.5 (0.3)	45 (10)	80 (22)
21	0.7 (0.06)	50 (6)	60 (15)
22	17 (5)	54 (5)	>500
23	0.4 (0.1)	87 (5)	15 (4)
24	10.0 (0.3)	50 (1)	164 (24)
25	4.2 (0.3)	48 (10)	79 (22)
26	3.4 (0.3)	69 (2)	58 (10)
27	5.5 (0.8)	52 (7)	450 (75)
28	4.2 (0.7)	31 (3)	>1000
29	45 (9)	40 (3)	>1000
30	0.32 (0.06)	100 (8)	4.2 (0.6)
31	1.1 (0.2)	93 (4)	25 (6)
32	8 (1)	76 (5)	350 (7)
33	6.2 (0.7)	83 (5)	138 (21)
34	14 (1)	86 (3)	>500

Note. All values are expressed as mean ± SEM of at least three separate assays performed in duplicate.

acceptors are not well tolerated in Region A. Interestingly, in comparison to **7** and **22**, compound **6** (furanyl fentanyl) showed that aromaticity in Region A formed favorable interactions in the orthosteric binding site of hMOR (1.3nM).

Modifications at Region B (**23–29**, Table 2) compared both a halogen and a methyl substituent at the *ortho*, *meta*, and *para* positions. A

chlorine in the *para* position of Region B drastically decreased hMOR binding (45nM; *para*-chloro fentanyl, **29**), whereas a *para*-methyl did not (4.2nM; *para*-methyl fentanyl, **28**), suggesting a complex interaction between electronics and bulk. The relatively low EC_{50} potency seen in **29** (>1000nM) is consistent with previous mouse ED_{50} data.[24] This trend appears to be further demonstrated with *para*-chloro iso-butyryl fentanyl (**18**), which shows a greater-than-50-fold decrease in binding affinity compared to fentanyl (**1**) (82nM versus 1.6nM). In addition, the EC_{50} of **18** (>2000nM) is greater than 60-fold less potent than fentanyl (**1**) at hMOR. These data suggest that a large halogen substituent at the *para* position of Region B has a weakening effect on binding affinity and potency. The addition of a fluorine in the *meta* or *para* position on the aniline ring of Region B tends to decrease potency and efficacy at hMOR. In contrast, the addition of a fluorine in the *ortho* position increases potency and efficacy at hMOR (**1** versus **23**, **11** versus **12**, **14** versus **15**, and **20** versus **21**). This suggests that electronic density of the aromatic ring in Region B is important for making contact with the active conformation of hMOR. An *ortho*-fluorine in Region B increases the agonist character of fentalogs in all instances.

TABLE 3 GC–MS fragmentation of fentalogs

Compound #	RT (min.)	Base peak (*m/z*)	Fragmentation (*m/z*)	EC50 (SEM) nM
18	12.79	293	43, 180, 223, 293	>2000
7	14.41	287	71, 146, 189, 287	390 (96)
5	13.92	285	69, 146, 189, 285	600 (190)
29	12.88	279	57, 180, 223, 279	>1000
15	11.32	277	43, 164, 207, 277	42 (13)
16	11.06	277	43, 164, 207, 277	>500
21	11.82	277	43, 164, 207, 277	60 (15)
17	11.85	273	105, 160, 203, 273	>1000
3	12.84	271	69, 160, 203, 271	>1000
4	13.24	271	55, 146, 189, 271	160 (30)
23	11.57	263	57, 164, 207, 263	15 (4)
24	11.39	263	57, 164, 207, 263	164 (24)
25	11.39	263	57, 164, 207, 263	79 (22)
12	11.72	261	55, 164, 218, 261	14 (1)
13	11.48	261	55, 164, 218, 261	84 (11)
22	12.48	261	45, 105, 158, 261	>500
14	11.49	259	43, 146, 189, 259	137 (13)
20	11.83	259	105, 146, 189, 259	80 (22)
26	12.08	259	91, 160, 203, 259	58 (10)
27	11.84	259	91, 160, 203, 259	450 (75)
28	12.29	259	105, 160, 203, 259	>1000
30	11.78	259	105, 160, 203, 259	4.2 (0.6)
31	11.66	259	91, 105, 160, 259	25 (6)
2	12.44	257	69, 146, 189, 257	55 (10)
Fentanyl (1)	11.80	245	91, 146, 189, 245	32 (8)
9	11.67	245	91, 160, 202, 245	>1000
10	11.57	245	56, 91, 110, 245	>500
32	10.85	245	57, 146, 189, 245	350 (7)
33	13.21	245	93, 146, 189, 245	138 (21)
34	11.53	245	91, 146, 189, 245	>500
11	11.73	243	55, 146, 200, 243	68 (16)
8	10.72	231	91, 146, 188, 231	>2000
6	14.24	95	95, 187, 240, 283	9.3 (1.9)
19	11.87	57	57, 105, 146, 273	531 (136)

Note. Parent compounds and their fragments are organized in order of descending base peak number. Red highlights the fluorinated analogs with the *m/z* 164 fragment.

Abbreviations: GC–MS, gas chromatography–mass spectrometry; RT, retention time.

Modifications at Region C have been studied extensively using *in vivo* and *in vitro* rodent models, which contain a subset of highly hazardous fentalogs, including 3- and 4-position substituted analogs such as carfentanil, ohmefentanyl, and enantiomerically pure (+)-*cis*-3-methyl fentanyl.[48-50] In this study, (+/−)-*cis*-3-methyl fentanyl (**30**) was used in an attempt to better emulate what may be found on the illicit market. As expected, compound **30** demonstrated a fivefold higher affinity for hMOR than fentanyl (**1**) (0.3nM versus 1.6nM). Other modifications in Region C (**31–34**), did not dramatically alter binding affinity at hMOR; the greatest deviation from fentanyl (**1**) was seen in β-methyl fentanyl (**34**), which displayed an almost 10-fold decrease in affinity (14nM). These data further confirm that substitutions on the piperidine ring yield the greatest binding affinity and potency increases in the samples tested.

3.2 | Structural analysis through GC–MS

The mass spectral fragmentation of fentanyl and many of its analogs has been previously reported.[51-54] Much attention has been paid to the interpretation of electron ionization-mass spectrometry (EI-MS) due to the routine use of GC–MS in forensic labs. The four most abundant EI-MS fragment ions in the GC–MS of the fentalogs in this study are listed in Table 3. As expected, and as previously reported, the base peak is typically the result of α-β cleavage of the phenethyl C–C bond (Region C).[55-57] In fentanyl (**1**), the base peak is *m/z* 245. Consistent with previous findings was the further fragmentation of the base peak yielding the characteristic 189 and 146 fragment ions as shown in Figure 2A.[55-58] The presence of the *m/z* 189, 146, and 91 fragments yields structural information as to where new fentanyl analogues may or may not have been modified.

Of the 34 fentalogs evaluated, *m/z* 245 and *m/z* 259 were the most commonly observed base peaks with the base peak 259 representing the substitution of an H for a CH_3 (methyl) as shown in Figure 2B (additional CH_3 shown in blue). The base peak *m/z* 259 is observed in compounds **14**, **20**, **26–28**, **30**, and **31**.

One notable observation in the EI-MS data of the fentalogs tested is the presence of the *m/z* 164 fragment, which indicates that a single fluorine has been installed on the fentanyl scaffold (depicted in red, Figure 2C and Table 3). All of the studied fentalogs producing the *m/z* 164 fragment (**12–13**, **15–16**, **21**, and **23–25**) displayed EC$_{50}$s of less than 100nM and/or > 80% G protein stimulation at hMOR (Table 2). This is consistent with literature reports of other fluorinated fentalogs, such as NFEPP, which contains a fluorine in the 3-position on the piperidine ring and has been reported to be a highly potent MOR agonist.[59] The observed correlation between the addition of a fluorine (at either Region B or the 3-position in Region C) with high potency at MOR highlights the need to carefully handle fentalogs containing a *m/z* 164 fragment ion.

Although it is a rapid means of identification, GC–MS is not the only analytical technique that can be used to identify fentalogs; ^{1}H- and ^{13}C-NMR spectroscopy can also be used to survey unknown samples for the presence of common fentalogs of abuse.

3.3 | Structural analysis through ^{1}H-NMR spectroscopy

Although the ^{1}H-NMR spectra of the studied fentalogs displayed many variances in both the aromatic and aliphatic regions, the spectra showed commonalities that were characteristic among a majority of the fentalogs tested.[60] The most notable characteristic peak among all of the fentalogs was a triplet of triplets (most often viewed as
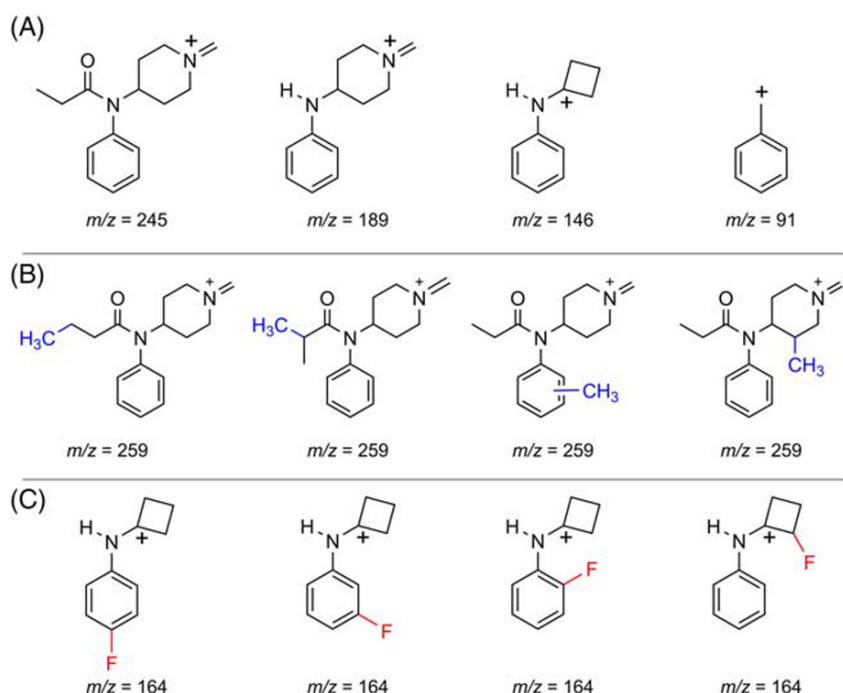

FIGURE 2 (A) Key fentanyl fragment ions. (B) Base peak fragment ions from fentalogs with the addition of a methyl group relative to fentanyl. (C) Possible structures of *m/z* 164 fragment

multiplet), positioned between 4.65 and 4.85 ppm. This peak represents the single proton on the 4-position of the piperidine ring and is present in all fentalogs in this study (supporting information). Further upfield, a group of four signals including two broad doublets (1.9 and 3.0 ppm), a broad triplet (2.2 ppm), and a quartet of doublets (1.5 ppm) can be seen and distinguished in most cases. These each integrate to two protons and indicate the eight protons associated with the piperidine ring, excluding the 4-position. There is also a set of mirror image multiplets (2.55–2.78 ppm), which is characteristic of the four protons on the phenethyl chain (α/β positions in Region C). Chemical shifts of all fentalogs included in this study can be found in the supporting information section as well as corresponding ^{13}C-NMR data.

4 | CONCLUSIONS

In this report we describe the spectroscopic analysis and *in vitro* pharmacology of a series of fentalogs. The pharmacological data presented in this report describe the structural features that convey potent hMOR agonism on the fentanyl scaffold, which could aid in predicting relative potencies of new analogs. In general, it should be noted that compounds containing an *ortho*-fluoro substituent in Region B display strong agonist character at hMOR and could be especially hazardous upon exposure.

Both binding affinity and potency are affected by the size of substitutions in Region A. Compounds that have very large or very small Region A moieties tend to have lower affinity and potency, suggesting that the parent scaffold that contains an ethyl group in Region A provides optimal contact with the active conformation of hMOR. Both the sterics and electron density of the Region B substituent impact the affinity and agonist activity of fentalogs. Compounds with *ortho*-fluoro substitutions in Region B showed improved binding affinity and efficacy at MOR as compared to fentanyl, making them potentially hazardous, whereas *para*-chloro substituents decreased potency.

The GC–MS analysis highlighted the common molecular ion fragments of *m/z* 146 and *m/z* 189 that indicate many fentalogs. All potent fentalogs with a *m/z* 164 fragment ion contained a fluorine in Region B or the piperidine ring of Region C. In addition, the ^{1}H-NMR analysis demonstrated shared coupling and splitting patterns in the aliphatic region among all fentalogs tested, which can be used for identification and differentiation of fentalogs in unknown samples.

Taken together, these data may help to guide government regulating bodies and law enforcement communities in identifying fentalogs in unknown samples as well as aid in safe handling practices when encountering potential high-potency analogs. This information has the potential to aid in rational scheduling of fentalog structures and inform guidelines for overdose treatment in case of exposure.

AUTHOR CONTRIBUTIONS
S.H.H., J.R.B., and the Dept. of Forensic Chemistry (Cayman Chemical) synthesized and characterized the fentalog compounds in this report. Pharmacological assays were performed by C.M.P.N, J.J.T., and J.P.A. (Dept. of Pharmacology, University of Michigan). Pharmacological assays were designed and interpreted by J.P.A. and J.R.T (Dept. of Pharmacology, University of Michigan). Manuscript was prepared by S.H.H., J.R.B., D.M.I., J.R.T., and J.P.A.

ORCID
Sherif H. Hassanien https://orcid.org/0000-0001-6507-1166
Jessica P. Anand https://orcid.org/0000-0001-6560-2211

REFERENCES
1. Schuchat A, Houry D, Guy GP Jr. New data on opioid use and prescribing in the United States. *JAMA*. 2017;318(5):425-426. https://doi.org/10.1001/jama.2017.8913
2. Compton WM, Volkow ND. Major increases in opioid analgesic abuse in the United States: concerns and strategies. *Drug and Alcohol Depend*. 2006;81(2):103-107. https://doi.org/10.1016/j.drugalcdep.2005.05.009
3. Volkow ND, Jones EB, Einstein EB, Wargo EM. Prevention and treatment of opioid misuse and addiction: a review. *JAMA Psychiat*. 2019;76(2):208-216. https://doi.org/10.1001/jamapsychiatry.2018.3126
4. Florence CS, Zhou C, Luo F, Xu L. The economic burden of prescription opioid overdose, abuse, and dependence in the United States, 2013. *Med Care*. 2016;54(10):901-906. https://doi.org/10.1097/mlr.0000000000000625
5. Oderda GM, Lake J, Rüdell K, Roland CL, Masters ET. Economic burden of prescription opioid misuse and abuse: a systematic review. *J Pain Palliat Care Pharmacother*. 2015;29(4):388-400. https://doi.org/10.3109/15360288.2015.1101641
6. Murthy VH. Facing addiction in the United States: the surgeon General's report of alcohol, drugs, and health. *JAMA*. 2017;317(2):133-134. https://doi.org/10.1001/jama.2016.18215
7. Scholl L, Seth P, Kariisa M, Wilson N, Baldwin G. Drug and opioid-involved overdose deaths - United States, 2013–2017. *MMWR Morb Mortal Wkly Rep*. 2018;67(5152):1419-1427. https://doi.org/10.15585/mmwr.mm675152e1
8. National Highway Traffic Safety Administration. Traffic safety facts research note: 2017 fatal motor vehicle crashes: overview. https://crashstats.nhtsa.dot.gov/Api/Public/ViewPublication/812603. Accessed November 11th, 2019.
9. American Society of Actuaries. Economic Impact of Non-Medical Opioid Use in the United States, 2019. https://www.soa.org/globalassets/assets/files/resources/research-report/2019/econ-impact-non-medical-opioid-use.pdf. Accessed April 26th, 2020.
10. Rudd RA, Paulozzi LJ, Bauer MJ, et al. Increases in heroin overdose deaths - 28 states, 2010 to 2012. *MMWR Morb Mortal Wkly Rep*. 2014;63(39):849-854.
11. Marinetti LJ, Ehlers BJ. A series of forensic toxicology and drug seizure cases involving illicit fentanyl alone and in combination with heroin, cocaine or heroin and cocaine. *J Anal Toxicol*. 2014;38(8):592-598. https://doi.org/10.1093/jat/bku086
12. Seth P, Rudd RA, Noonan RK, Haegerich TM. Quantifying the epidemic of prescription opioid overdose deaths. *Am J Public Health*. 2018;108(4):500-502. https://doi.org/10.2105/AJPH.2017.304265

13. National Center for Health Statistics. NCHS Data Brief: Drug overdose deaths in the United States, 1999–2017. - 2017. Issue 329. https://www.cdc.gov/nchs/data/databriefs/db329-h.pdf. Accessed November 11th, 2019.

14. United States Drug Enforcement Administration. 2017 National Drug Threat Assessment. https://www.dea.gov/sites/default/files/2018-07/DIR-040-17_2017-NDTA.pdf. Accessed Novermber 11th, 2019.

15. Mignat C, Wille U, Ziegler A. Affinity profiles of morphine, codeine, dihydrocodeine and their glucuronides at opioid receptor subtypes. *Life Sci*. 1995;56(10):793-799. https://doi.org/10.1016/0024-3205(95)00010-4

16. Inturrisi CE, Schultz M, Shin S, Umans JG, Angel L, Simon EJ. Evidence from opiate binding studies that heroin acts through its metabolites. *Life Sci*. 1983;33(1):773-776. https://doi.org/10.1016/0024-3205(83)90616-1

17. Selley DE, Cao C-C, Sexton T, Schwegel JA, Martin TJ, Childers SR. μ opioid receptor-mediated G-protein activation by heroin metabolites: evidence for greater efficacy of 6-monoacetylmorphine compared with morphine. *Biochem Pharmacol*. 2001;62(4):447-455. https://doi.org/10.1016/S0006-2952(01)00689-X

18. Dahan A, Aarts L, Smith TW. Incidence, reversal, and prevention of opioid-induced respiratory depression. *Anesthesiology*. 2010;112(1):226-238. https://doi.org/10.1097/ALN.0b013e3181c38c25

19. Contet C, Kieffer BL, Befort K. Mu opioid receptor: a gateway to drug addiction. *Curr Opin Neurobiol*. 2004;14(3):370-378. https://doi.org/10.1016/j.conb.2004.05.005

20. Al-Hasani R, Bruchas MR. Molecular mechanisms of opioid receptor-dependent signaling and behavior. *Anesthesiology*. 2011;115(6):1363-1381. https://doi.org/10.1097/ALN.0b013e318238bba6

21. Romberg R, Sarton E, Teppema L, Matthes HWD, Kieffer BL, Dahan A. Comparison of morphine-6-glucuronide and morphine on respiratory depressant and antinociceptive responses in wild type and μ-opioid receptor deficient mice. *Br J Anaesth*. 2003;91(6):862-870. https://doi.org/10.1093/bja/aeg279

22. Hill R, Santhakumar R, Dewey W, Kelly E, Henderson G. Fentanyl depression of respiration: comparison with heroin and morphine. *Br J Pharmacol*. 2019;254–265. https://doi.org/10.1111/bph.14860

23. Torralva R, Janowsky A. Noradrenergic mechanisms in fentanyl-mediated rapid death explain failure of naloxone in the opioid crisis. *J Pharmacol Exp Ther*. 2019;371(2):453-475. https://doi.org/10.1124/jpet.119.258566

24. Higashikawa Y, Suzuki S. Studies on 1-(2-phenethyl)-4-(N-propionylanilino)piperidine (fentanyl) and its related compounds. VI. Structure-analgesic activity relationship for fentanyl, methyl-substituted fentanyls and other analogues. *Forensic Toxicol*. 2008;26(1):1-5. https://doi.org/10.1007/s11419-007-0039-1

25. Maryanoff BE, Simon EJ, Gioannini T, Gorissen H. Potential affinity labels for the opiate receptor based on fentanyl and related compounds. *J Med Chem*. 1982;25(8):913-919. https://doi.org/10.1021/jm00350a006

26. Lobbezoo MW, Soudijn W, van Wijngaarden I. Opiate receptor interaction of compounds derived from or structurally related to fentanyl. *J Med Chem*. 1981;24(7):777-782. https://doi.org/10.1021/jm00139a003

27. Brine GA, Stark PA, Liu Y, et al. Enantiomers of Diastereomeric cis-N-[1-(2-Hydroxy-2-phenylethyl)-3-methyl-4-piperidyl]-N-phenylpropanamides: synthesis, X-ray analysis, and biological activities. *J Med Chem*. 1995;38(9):1547-1557. https://doi.org/10.1021/jm00009a015

28. Rothman RB, Heng X, Seggel M, et al. RTI-4614-4: an analog of (+)-cis-3-methylfentanyl with a 27,000-fold binding selectivity for mu versus delta opioid binding sites. *Life Sci*. 1991;48(23):PL111-PL116. https://doi.org/10.1016/0024-3205(91)90346-D

29. Alburges ME, Hanson GR, Gibb JW, Sakashita CO, Rollins DE. Fentanyl receptor assay II. Utilization of a Radioreceptor assay for the analysis of fentanyl analogs in urine. *J Anal Toxicol*. 1992;16(1):36-41. https://doi.org/10.1093/jat/16.1.36

30. Wilde M, Pichini S, Pacifici R, et al. Metabolic pathways and potencies of new fentanyl analogs. *Front Pharmacol*. 2019;10:238. https://doi.org/10.3389/fphar.2019.00238

31. WHO Expert Committee of Drug Dependence (ECDD). Acetylfentanyl Critical Review Report 2015. https://www.who.int/medicines/access/controlled-substances/5.2_Acetylfentanyl_CRev.pdf. Accessed April 26th, 2020.

32. WHO Expert Committee of Drug Dependence (ECDD). Butyrfentanyl (Butyrylfentanyl) Critical Review Report 2016. https://www.who.int/medicines/access/controlled-substances/4.2_Butyrfentanyl_CritReview.pdf. Accessed April 26th, 2020.

33. WHO Expert Committee of Drug Dependence (ECDD). 4-Fluoroisobutyrylfentanyl (4-FIBF) Crtical Review Report 2017. https://www.who.int/medicines/access/controlled-substances/CriticalReview_4FIBF.pdf. Accessed April 26th, 2020.

34. WHO Expert Committee of Drug Dependence (ECDD). Acrylorylfentanyl Critical Review Report 2017. https://www.who.int/medicines/access/controlled-substances/CriticalReview_Acrylolyfentanyl.pdf. Accessed April 26th, 2020.

35. WHO Expert Committee of Drug Dependence (ECDD). Furanyl Fentanyl Critical Review Report 2017. https://www.who.int/medicines/access/controlled-substances/CriticalReview_FuranylFentanyl.pdf. Accessed April 26th, 2020.

36. WHO Expert Committee of Drug Dependence (ECDD). Tetra-hydrofuranyl fentanyl (THF-F) Critical Review Report 2017. https://www.who.int/medicines/access/controlled-substances/CriticalReview_THFF.pdf. Accessed April 26th, 2020.

37. WHO Expert Committee of Drug Dependence (ECDD). Critical Review Report: Cyclopropylfentanyl 2018. https://www.who.int/medicines/access/controlled-substances/Cyclopropylfentanyl.pdf. Accessed April 26th, 2020.

38. WHO Expert Committee of Drug Dependence (ECDD). Critical Review Report: Methoxyacetyl Fentanyl 2018. https://www.who.int/medicines/access/controlled-substances/Methoxyacetylfentanyl.pdf. Accessed April 26th, 2020.

39. WHO Expert Committee of Drug Dependence (ECDD). Critical Review Report: orthofluorofentanyl 2018. https://www.who.int/medicines/access/controlled-substances/Orthofluorofentanyl.pdf. Acccessed April 26th, 2020.

40. Cannaert A, Vasudevan L, Friscia M, Mohr ALA, Wille SMR, Stove CP. Activity-based concept to screen biological matrices for opiates and (synthetic) opioids. *Clin Chem*. 2018;64(8):1221-1229. https://doi.org/10.1373/clinchem.2018.289496

41. Alarcon K, Martz A, Mony L, et al. Reactive derivatives for affinity labeling in the ifenprodil site of NMDA receptors. *Bioorg Med Chem Lett*. 2008;18(9):2765-2770. https://doi.org/10.1016/j.bmcl.2008.04.019

42. Qin Y, Ni L, Shi J, et al. Synthesis and biological evaluation of fentanyl analogues modified at phenyl groups with alkyls. *ACS Chem Nerosci*. 2019;10(1):201-208. https://doi.org/10.1021/acschemneuro.8b00363

43. Toll L, Berzetei-Gurske IP, Polgar WE, et al. Standard binding and functional assays related to medications development division testing for potential cocaine and opiate narcotic treatment medications. *NIDA Res Monogr*. 1998;178:440-466.

44. Yung-Chi C, Prusoff WH. Relationship between the inhibition constant (KI) and the concentration of inhibitor which causes 50 per cent inhibition (I50) of an enzymatic reaction. *Biochem Pharmacol*. 1973;22(23):3099-3108. https://doi.org/10.1016/0006-2952(73)90196-2

45. Yeadon M, Kitchen I. Differences in the characteristics of opioid receptor binding in the rat and marmoset. *J Pharm Pharmacol*. 1988;40(10):736-739. https://doi.org/10.1111/j.2042-7158.1988.tb07008.x

46. Volpe DA, McMahon Tobin GA, Mellon RD, et al. Uniform assessment and ranking of opioid mu receptor binding constants for selected opioid drugs. *Regul Toxicol Pharmacol.* 2011;59(3):385-390. https://doi.org/10.1016/j.yrtph.2010.12.007

47. Xu H, Kim CH, Zhu YC, et al. (+)-cis-3-Methylfentanyl and its analogs bind pseudoirreversibly to the mu opioid binding site: evidence for pseudoallosteric modulation. *Neuropharmacology.* 1991;30(5):455-462. https://doi.org/10.1016/0028-3908(91)90006-W

48. Titeler M, Lyon RA, Kuhar MJ, et al. μ opiate receptors are selectively labelled by [³H]carfentanil in human and rat brain. *Eur J Pharmacol.* 1989;167(2):221-228. https://doi.org/10.1016/0014-2999(89)90582-7

49. Band L, Xu H, Bykov V, et al. The potent opioid agonist, (+)-cis-3-methylfentanyl binds pseudoirreversibly to the opioid receptor complex *in vitro* and *in vivo*: evidence for a novel mechanism of action. *Life Sci.* 1990;47(24):2231-2240. https://doi.org/10.1016/0024-3205(90)90154-J

50. Cheng MT, Kruppa GH, McLafferty FW, Cooper DA. Structural information from tandem mass spectrometry for China white and related fentanyl derivatives. *Anal Chem.* 1982;54(13):2204-2207. https://doi.org/10.1021/ac00250a016

51. Watanabe S, Vikingsson S, Roman M, Green H, Kronstrand R, Wohlfarth A. In vitro and in vivo metabolite identification studies for the new synthetic opioids Acetylfentanyl, Acrylfentanyl, Furanylfentanyl, and 4-Fluoro-Isobutyrylfentanyl. *AAPS j.* 2017;19(4):1102-1122. https://doi.org/10.1208/s12248-017-0070-z

52. Åstrand A, Töreskog A, Watanabe S, Kronstrand R, Gréen H, Vikingsson S. Correlations between metabolism and structural elements of the alicyclic fentanyl analogs cyclopropyl fentanyl, cyclobutyl fentanyl, cyclopentyl fentanyl, cyclohexyl fentanyl and 2,2,3,3-tetramethylcyclopropyl fentanyl studied by human hepatocytes and LC-QTOF-MS. *Arch Toxicol.* 2019;93(1):95-106. https://doi.org/10.1007/s00204-018-2330-9

53. Moore JM, Allen AC, Cooper DA, Carr SM. Determination of fentanyl and related compounds by capillary gas chromatography with electron capture detection. *Anal Chem.* 1986;58(8):1656-1660. https://doi.org/10.1021/ac00121a013

54. Ohta H, Suzuki S, Ogasawara K. Studies on fentanyl and related compounds IV. Chromatographic and spectrometric discrimination of fentanyl and its derivatives. *J Anal Toxicol.* 1999;23(4):280-285. https://doi.org/10.1093/jat/23.4.280

55. Breindahl T, Kimergård A, Andreasen MF, Pedersen DS. Identification of a new psychoactive substance in seized material: the synthetic opioid N-phenyl-N-[1-(2-phenethyl)piperidin-4-yl]prop-2-enamide (Acrylfentanyl). *Drug Test Anal.* 2017;9(3):415-422. https://doi.org/10.1002/dta.2046

56. Pierzynski H, Neurbauer L, Choi C. Cayman Currents: Fentanyl Identification. 2017. https://www.caymanchem.com/cms/caymanchem/LiteratureCMS/800181.pdf. Accessed November 11ᵗʰ, 2019.

57. Goromaru T, Katashima M, Matsuura H, Yoshimura N. Metabolism of fentanyl in isolated hepatocytes from rat and Guinea pig. *Chem Pharm Bull (Tokyo).* 1985;33(9):3922-3928.

58. Spahn V, Del Vecchio G, Labuz D, et al. A nontoxic pain killer designed by modeling of pathological receptor conformations. *Science.* 2017;355(6328):966-969. https://doi.org/10.1126/science.aai8636

59. Duffy J, Urbas A, Niemitz M, Lippa K, Marginean I. Differentiation of fentanyl analogues by low-field NMR spectroscopy. *Anal Chim Acta.* 2019;1049:161-169. https://doi.org/10.1016/j.aca.2018.12.014

60. Vasudevan L, Vandeputte M, Deventer M, Wouters E, Cannaert A, Stove CP. Assessment of structure-activity relationships and biased agonism at the Mu opioid receptor of novel synthetic opioids using a novel, stable bio-assay platform. *Biochem Pharmacol.* 2020;177 113910https://doi.org/10.1016/j.bcp.2020.113910

SUPPORTING INFORMATION

Additional supporting information may be found online in the Supporting Information section at the end of this article.